Noncovalent functionalization of carbon nanotubes and graphene with tetraphenylporphyrins: Stability and optical properties from *ab-initio* calculations

Walter Orellana*
Departamento de Ciencias Físicas, Universidad Andres Bello, República 220, 837-0134 Santiago, Chile

J. D. Correa
Departamento de Ciencias Básicas, Universidad de Medellín, Medellín, Colombia

(Dated: October 15, 2014)

The stability, electronic and optical properties of single-walled carbon nanotubes (CNTs) and graphene noncovalently functionalized with free-base tetraphenylporphyrin (TPP) molecules is addressed by density functional theory calculations, including corrections to dispersive interactions. We study the TPP physisorption on 42 CNT species, particularly those with chiral indices (n,m), where $5 \leq n \leq 12$ and $0 \leq m \leq n$. Our results show a quite strong π-π interaction between TPP and the CNT surface, with binding energies ranging from 1.1 to 1.8 eV, where higher energies can be associated with increasing CNT diameters. We also find that the TPP optical absorptions would not be affected by the CNT diameter or chirality. Results for the TPP physisorption on graphene show a remarkable stability with binding energy of 3.2 eV, inducing a small redshift on the π-stacked TPP absorption bands. The strong graphene-TPP interaction also induces a charge transfer from TPP to graphene, indicating a n-type doping mechanism without compromising the graphene structure.

I. INTRODUCTION

Noncovalent functionalization of single-walled carbon nanotubes (CNTs) with photoactive molecules is becoming a promising technique to explore functional materials for light-harvesting or optoelectronic applications.[1–8] The coupling of the exceptional CNT transport properties with the optical properties of functional dyes, like porphyrins with a strong absorption in the near infrared and visible, make of CNT/dye complexes good candidates for sensitive nanoscale devices with potential applications in biomedical imaging,[9–11] and hybrid organic-inorganic photovoltaic devices.[12] However, the strength of the π-stacking interaction with respect to the CNT structural parameters, like the diameter and chirality, is still lacking. In addition, a better understanding of the CNT/dye optical properties considering changes in the dye structure due to the π-conjugation is needed.

Recently, the kinetics and thermodynamics properties of non-covalently bound CNT/porphyrin oligomers have been investigated by UV/visible spectroscopy and fluorescence titration.[13] It was reported that the affinity of the CNTs increases sharply with the porphyrin coverage, showing strongest binding energies for semiconducting CNTs, particularly those with chiral indices (7,5) and (8,6). In addition, others works have also investigated a supposed selective interaction of porphyrins towards semiconducting CNTs, suggesting that the semiconducting and metallic CNTs would have significantly different surface properties.[14,15] These works have also suggested that noncovalent functionalization of a mixture of CNTs with porphyrins may be an effective method for the separation of semiconducting CNTs from metallic CNTs. Previously, we reported physisorption properties of iron porphyrin on both metallic and semiconducting CNTs with similar diameters.[16] Our results showed a surprising strong π-stacking interaction, but with negligible energy differences. Similar results were found for the physisorption strength of free-base and zinc porphyrins on the same semiconducting CNT,[17,18] showing no clue on the suspected selectivity.

Considering the increasing interest in the noncovalent complexation of CNT-based materials for optoelectronic applications, we carry out an in-depth investigation on the stability and optical response of free-base tetraphenyporphyrin (TPP) molecules π-stacked on single-walled CNTs with different chiralities and diameters, and also on graphene. Our purpose is to give a theoretically insight into the binding strength and optical properties of these compounds as a function of the CNT structural parameters. Our results show that the diameter instead chirality would be the relevant CNT parameter to explain the unusual strength of the TPP π-stacking interaction. In addition, the TPP binding energy on metallic and semiconducting CNTs does not exhibit important differences that might suggest distinct interactions. Regarding optical properties, we find that transition bands of the π-stacked TPP remain at almost the same energy position than those found in the isolated TPP, being independent of the CNT structural parameters. For the TPP physisorption on graphene, we find a very strong binding energy, of about 3.2 eV, providing an upper limit for the stability of CNT-TPP compounds. We also find a p-type doping on graphene induced by the TPP adsorption.

*E-mail: worellana@unab.cl

II. THEORETICAL APPROACH

Our density functional theory (DFT) calculations were performed using the SIESTA *ab initio* package,[19] which employ norm-conserving pseudopotentials and localized atomic orbitals as basis set (double-ζ, singly polarized). The physisorption of TPP on both the CNT sidewall and graphene is assessed by van der Waals density functional (vdW-DF) as proposed by Dion *et al.*[20] This approach has been successfully applied to describe the dispersive interaction of aromatic molecules on the graphite surface, showing good agreement with available experimental data.[21]

In recent experiments, the functionalization of CNTs with TPP molecules has been achieved by the micelle swelling methods in water suspension,[4] where the CNT-TPP compound stays in the micelle core. Because of the hydrophobic character of this core, it is not expected water molecules surrounding the compound, which can be considered close to a vacuum situation. In the present work we study the TPP physisorption 42 different CNT species, particularly those with chiral indices (n,m), with $5 \leq n \leq 12$ and $0 \leq m \leq n$. The CNT-TPP compounds are studied within the supercell approach, with periodic boundary conditions along the nanotube axis (z direction). We use unit cells with a volume of $(30\times30\times\ell a_0)$ Å^3, where a_0 is CNT lattice constant and ℓ a factor to keep a minimum distance among TPP images along the CNTs, chosen to be of 10 Å. This procedure results in supercell lengths (ℓa_0) between 22-57 Å, which can contain up to 754 atoms. A grid cutoff of 100 Ry and the Γ point were used for the real-space and k-space integration, respectively. For the optical calculations, we use a $1\times1\times31$ k-point mesh, for incident light polarized along the CNT axis. The accuracy of these parameters were tested considering larger grid cutoff (150 Ry) and k-point mesh ($1\times1\times10$). Negligible variations in the total energies, optical spectra, and band structures were found, ensuring that our results are converged. For the TPP physisorption on graphene, we use a squared unit cell with 6×6 periodicity and the Γ point for the k-space integration. Here, a vacuum region of 20 Å among graphene an their images was considered. For the optical response we use a k-point mesh of $31\times31\times1$, for incident light polarized parallel to the graphene plane (x and y directions). The TPP binding energy on the substrates is calculated by the energy difference between adsorbed and separated constituents, considering corrections due to the basis set superposition error. The complexes were fully relaxed by conjugate gradient minimization until the forces on the atoms were less than 0.05 eV/Å.

The optical response of the functionalized CNTs and graphene is obtained through first order time dependent perturbation theory, by calculating the imaginary part of the dielectric function (ε_2). ε_2 gives us a first approach for the optical absorption coefficient and it is calculated according to the equation:

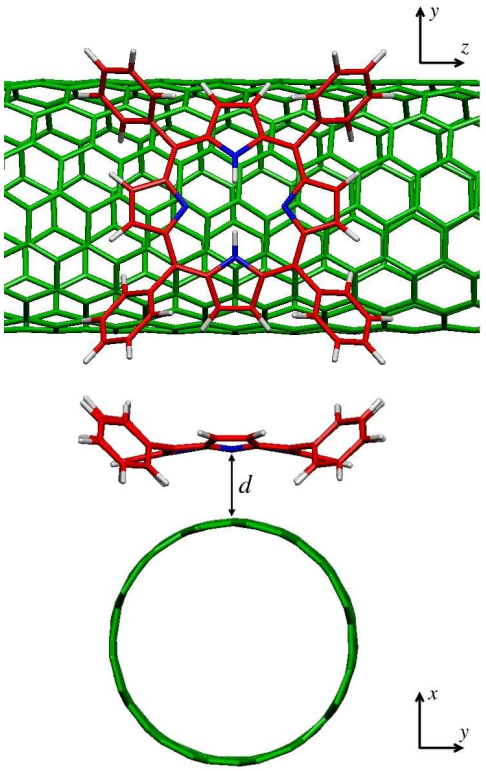

FIG. 1: Top and front views of a free-base tetraphenylporphyrin (TPP) physisorbed on the (8,7) CNT in the equilibrium geometry. Blue and white bars represent nitrogens and hydrogens, respectively, whereas green and red are carbons.

$$\varepsilon_2(\omega) = A\int d\mathbf{k}\sum_{c,v}\left|\hat{\epsilon}\cdot\langle\Psi_c(\mathbf{k})|\mathbf{r}|\Psi_v(\mathbf{k})\rangle\right|^2\delta(E_c-E_v-\hbar\omega). \quad (1)$$

Here A is a constant that depends on the cell sizes; Ψ_c and Ψ_v are the occupied and empty Kohn-Sham orbitals, respectively. The delta function represents the conservation of energy, which is described by a gaussian function with a smearing of 0.06 eV.

It is important to note that DFT calculations fail in describing electron-hole and electron-electron interactions, the so called many-body effects. These effects are responsible for the formation of excitons and the quasiparticle excitation.[22] Therefore, an accurate description of photoexcitations in CNTs and graphene needs theories beyond DFT, like those based on the GW-Bethe-Salpeter equation (GW-BSE).[23] However, these calculations are not possible right now, considering the size of the systems under study. Thus, ε_2 can give us a first approach for the optical response of π-stacked TPP on CNTs and graphene. The main difference of DFT calculations with respect to GW-BSE is a redshift in the absorption spectrum. For instance, in graphene this redshift is found to be about 0.6 eV.[22,24]

III. RESULTS AND DISCUSSION

A. Energetic and structural properties

We first discuss different adsorption geometries for the TPP molecule on the CNTs. Figure 1 shows the equilibrium geometry of a TPP adsorbed on a (8,7) CNT. Here, the N-H bonds of TPP are oriented perpendicular to the CNT axis, that we called position (i). Two other positions for TPP are likely to be found: with the N-H bonds parallel to the CNT axis (ii), and with the N-H bonds forming an angle of 45° with respect to the CNT axis (iii). Although position (i) is found to be the most stable, the other positions have total energies within 0.3 eV, suggesting that all three are equally probables. In the equilibrium geometry, the TPP phenyl groups exhibit a small rotation, which come with a molecular twisting. To compare the stability of different CNT-TPP complexes, only position (i) will be considered throughout this work. The adsorption distance is measured between the CNT surface and the N atoms of TPP, as shown in Figure 1. Table I lists TPP binding energies and binding distances for all the complex under study. We also include the DFT bandgaps for the semiconducting complexes. Those with small bandgaps (∼0.1 eV) are consistent with empirical model predictions of E_{11} as well as with experimental data.[25] We observe that binding energies and adsorption distances vary in ranges given by $1.1 \leq E_b \leq 1.8$ eV and $3.0 \leq d \leq 3.3$ Å, respectively. We note that stronger TPP π-stacking interactions result in larger adsorption distance. This can be understood by look at the TPP phenyl groups, whose H atoms become closer to the CNT surface for large diameter CNTs, as can be seen in Figure 1. To estimate an upper limit for E_b and d, we calculate the TPP physisorption on graphene, which can be considered as a CNT with an infinite diameter. We find $E_b = 3.32$ eV and $d = 3.42$ Å. Although the binding distance is similar to those found on CNTs with $D \leq 16$ Å, the binding energy is considerably larger, with almost twice the value found on the CNTs. This can be understood because of the larger graphene-TPP overlap area, which tend to maximize the π-stacking interaction.

Figure 2 shows the CNT-TPP binding energy as a function of the CNT diameter. We observe an almost linear increase in the TPP attachment strength with the CNT diameter, which in some way confirms our assumption that larger CNT-TPP overlap area tends to increase the binding energy of the molecule. However, this general tendency is not followed in some cases, as can be seen in Fig. 2. For instance, (i) the larger TPP binding energy found for the (5,0) CNT ($D = 4$ Å) with respect to the (6,0) CNT ($D = 5$ Å), by about 0.2 eV, and (ii) the abrupt changes in the TPP binding energy profile going from (6,0) to (6,1), (7,5) to (7,6), and (8,5) to (8,6). We attribute these results to the particular atomic geometry of the CNT atoms just below the TPP molecule. We observe that the CNT-TPP binding distance tends to increase when the H atoms of the phenyl groups nearest neighbors to the CNT surface, lie exactly above nanotube C-atoms. This effect is due to the steric repulsion between them, which also explain the broad variation on the binding distances between the CNT surface and the TPP N-atoms, as shown in Figure 3.

Figure 4 shows the CNT-TPP binding energy as a function of the CNT chiral angle. Apparently, higher chiral angles would induce stronger TPP attachment. However, if we compare the TPP attachment on CNTs with

TABLE I: Adsorption distance (d), binding energy (E_b), and bandgap energy (E_g) of CNT-TPP complexes. D and θ_c are the CNT diameter and chiral angle, respectively. Results for TPP on graphene (G-TPP) are also included.

Complex	D(Å)	θ_c(deg)	E_g(eV)	d(Å)	E_b(eV)
(5,0)-TPP	3.902	0.0	0.19	3.000	1.22
(5,1)-TPP	4.526	8.9	0.00	3.052	1.17
(5,2)-TPP	5.083	16.1	0.00	3.106	1.18
(5,3)-TPP	5.686	21.8	1.15	3.124	1.25
(5,4)-TPP	6.315	26.3	1.04	3.142	1.25
(5,5)-TPP	7.055	30.0	0.00	3.064	1.35
(6,0)-TPP	4.921	0.0	0.00	3.117	1.11
(6,1)-TPP	5.118	7.6	0.40	3.084	1.24
(6,2)-TPP	5.837	13.9	0.67	3.116	1.21
(6,3)-TPP	6.401	19.1	0.02	3.180	1.21
(6,4)-TPP	7.025	23.4	1.02	3.079	1.35
(6,5)-TPP	7.704	27.0	0.87	3.161	1.36
(6,6)-TPP	8.362	30.0	0.00	3.114	1.39
(7,0)-TPP	5.685	0.0	0.24	3.091	1.18
(7,1)-TPP	6.115	6.6	0.00	3.056	1.23
(7,2)-TPP	6.608	12.2	0.84	3.134	1.25
(7,3)-TPP	7.165	17.0	0.86	3.183	1.24
(7,4)-TPP	7.754	21.1	0.03	3.166	1.35
(7,5)-TPP	8.372	24.5	0.85	3.138	1.42
(7,6)-TPP	9.038	27.5	0.75	3.142	1.50
(7,7)-TPP	9.703	30.0	0.00	3.182	1.48
(8,0)-TPP	6.468	0.0	0.60	3.159	1.30
(8,1)-TPP	6.511	5.8	0.78	3.106	1.35
(8,2)-TPP	7.384	10.9	0.09	3.143	1.37
(8,3)-TPP	7.934	15.3	0.96	3.211	1.40
(8,4)-TPP	8.490	19.1	0.77	3.163	1.45
(8,5)-TPP	9.103	22.4	0.02	3.192	1.46
(8,6)-TPP	9.749	25.3	0.74	3.298	1.35
(8,7)-TPP	10.410	27.8	0.66	3.197	1.42
(8,8)-TPP	11.105	30.0	0.00	3.110	1.54
(9,0)-TPP	7.269	0.0	0.15	3.213	1.33
(9,1)-TPP	7.685	5.2	1.01	3.145	1.28
(9,2)-TPP	8.165	9.8	0.73	3.248	1.44
(9,9)-TPP	12.467	30.0	0.00	3.205	1.54
(10,0)-TPP	8.027	0.0	0.74	3.179	1.41
(10,1)-TPP	8.458	4.7	0.06	3.100	1.44
(10,2)-TPP	8.938	8.9	0.85	3.126	1.44
(10,10)-TPP	13.929	30.0	0.00	3.222	1.59
(12,0)-TPP	9.638	0.0	0.10	3.180	1.46
(12,1)-TPP	10.042	4.0	0.77	3.163	1.50
(12,2)-TPP	10.495	7.6	0.61	3.123	1.49
(12,12)-TPP	16.634	30.0	0.00	3.180	1.82
G-TPP	∞	-	0.00	3.424	3.32

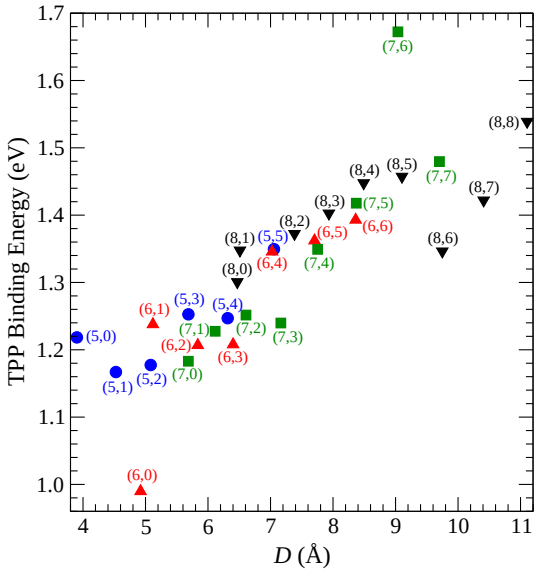

FIG. 2: Binding energy of a TPP molecule physisorbed on different CNTs as a function of the CNT diameter (D).

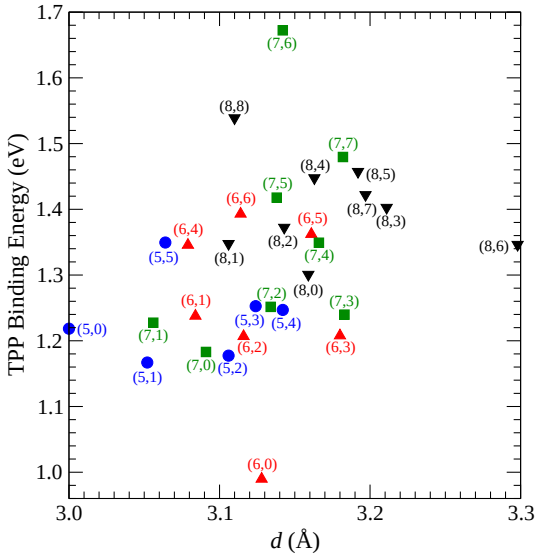

FIG. 3: Binding energy of a TPP molecule physisorbed on different CNTs as a function of the CNT-TPP binding distance (d).

similar diameters and binding distances with those plotted as a function of the chiral angle, we observe that they have also similar binding energy, suggesting that the CNT diameter instead chirality is the relevant parameter involved in the strong TPP binding energy. For instance, if we take the CNTs with chiral indices (5,4) and (7,2), they show almost the same TPP binding energy when plotted with respect to both the CNT diameter (Fig. 2) and adsorption distance (Fig. 3). However, they also show the same binding energy when plotted with respect to the chiral angle (Fig. 4). The same behavior can be verified for the pairs of CNTs (5,5)-(6,4) and (6,5)-(7,4).

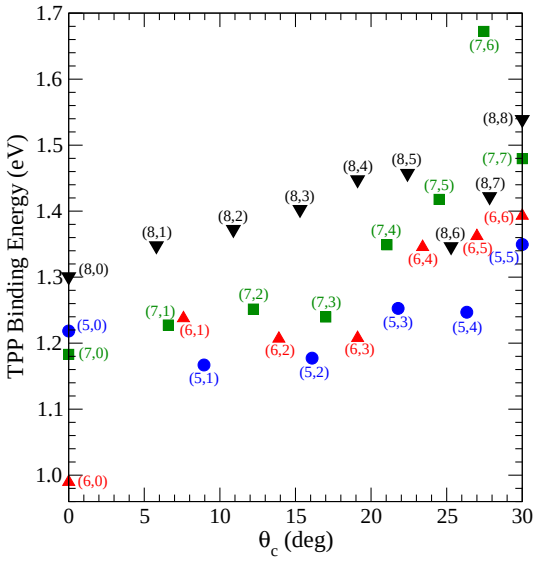

FIG. 4: Binding energy of a TPP molecule physisorbed on different CNTs as a function of the CNT chiral angle (θ_c).

These results suggest that the strength of the TPP interaction on the CNTs would not be related to the CNT surface geometry or chirality, but to the CNT diameter.

The adsorption energy of benzene and naphthalene on CNTs (7-8 Å diameter), using electron-correlated Moller-Plasset (MP2) method reports binding energies for benzene and naphthalene of 0.18 and 0.48 eV, respectively.[26] This results suggest an overestimation of the TPP adsorption energy on CNTs. However, temperature programmed desorption experiments performed in ultrahigh vacuum have measured the binding energy of polyaromatic hydrocarbons (PAHs) adsorbed on graphite, showing quite strong desorption energies.[27] In that work, benzene, naphthalene, coronene, and ovalene adsorbed on graphite show desorption energies of 0.50, 0.85, 1.4, and 2.1 eV, respectively. For the case of benzene and naphthalene, the experimental values almost double the MP2-theory values. Even considering the CNT curvatures, the π-stacking interaction appears to be much more larger than the usually expected. In addition, a recent study of PAHs adsorption on graphene shows that the vdW-DF calculations exhibit excellent agreement with the available experimental data, while empirical and semiempirical calculations only preserve the correct trends.[28] In summary, the work concludes that the adsorption interaction of π-conjugate systems on graphene are a complex combination of dispersive and electrostatic interactions, which would explains to some extent our results for the large adsorption energies of TPP on both graphene and CNTs.

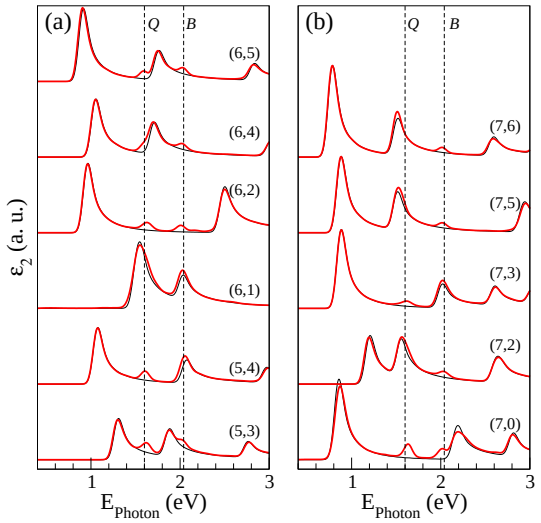

FIG. 5: Imaginary part of the dielectric function for semiconducting CNTs with a π-stacked TPP, for incident light polarized parallel to the tube axis. Red and black spectra indicate the optical response of CNT-TPP and the isolated CNT, respectively. The dashed lines indicate the position of Q and B bands of the isolated TPP.

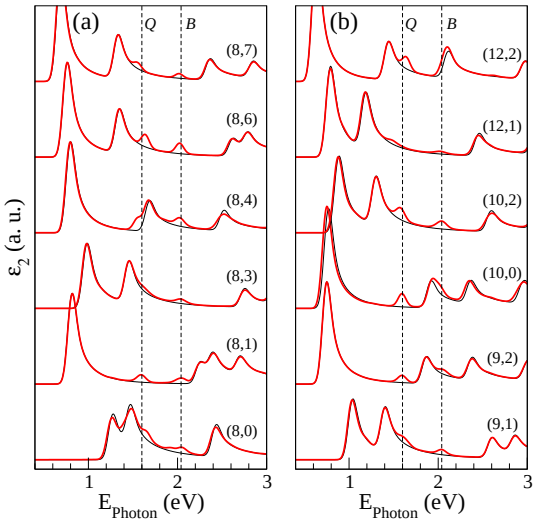

FIG. 6: Imaginary part of the dielectric function for semiconducting CNTs with a π-stacked TPP, for incident light polarized parallel to the tube axis. Red and black spectra indicate the optical response of CNT-TPP and the isolated CNT, respectively. The dashed lines indicate the position of Q and B bands of isolated TPP.

B. Optical properties

Noncovalent functionalization of a single-walled (6,5) CNT with TPP molecules have been reported in aqueous solution by mean of the micellar suspension method.[29] The optical absorption of (6,5)-TPP complexes shows resonances at 2.357 and 2.831 eV, which are associated to the Q and B (Soret) TPP bands, respectively.[4] Our results for the optical response of the (6,5)-TPP complex for a polarization parallel to the tube axis, show clear transitions at 1.60 and 2.04 eV, which we associate to the TPP Q and B bands, respectively. The difference in energy between these peaks (0.44 eV) is almost the same than those observed in the experiments (0.474 eV).[4] However, the theoretical peaks show a redshift of about 0.8 eV with respect to the experimental ones, while the shape of the absorption spectra would be preserved. This shift is associated to many-body effects previously discussed. Therefore, through the ε_2 calculation it is possible to investigate, qualitatively, changes in the optical properties of different CNT-TPP complexes in term of the CNT structural parameters, like diameter or chirality.

Figure 5 and 6 show ε_2 as a function of the photon energy, for incident light polarized parallel to the tube axis, for the semiconducting CNT-TPP complexes. The red and black spectra indicate the optical response of CNT-TPP and the isolated CNT, respectively. The vertical dashed lines indicate the position of the TPP Q (1.60 eV) and B (2.04 eV) bands. The optical spectra clearly show the absorption of the π-stacked TPP at almost the same position than the isolated TPP, indicating that the TPP absorption properties would be preserved in the complexes, being independent of the CNT diameter or chirality. However, we must note that the present results were obtained considering only one TPP molecule on the CNTs. Increasing TPP coverages may change this conclusion. The optical response of complexes considering metallic and semimetallic CNTs (not shown) exhibit the same properties. Another interesting feature is the resonance between the CNT E_{22} transition with the B band for the CNTs: (5,4), (6,1), (7,3), and (10,0), and with the Q band for the CNTs: (6,1), (7,5), (7,6), and (7,2). This tuning between E_{22} and the TPP bands would increase the emission of the corresponding complex.

Figure 7 shows the electronic band structure and density of states (DOS) of the graphene-TPP compound described in a squared reciprocal lattice. The vertical arrows show the optical transition between the frontier molecular orbitals of the π-stacked TPP, which correspond to the dispersionless subbands. Here, Q_x (Q_y) is the transition from HOMO to LUMO (LUMO+1), while B_x (B_y) is the transitions from HOMO-1 to LUMO (LUMO+1). These absorptions arise from $\pi - \pi^*$ transitions and can be characterized approximately by considering only the four molecular levels above mentioned.[17,31–33] In pristine graphene, the valence-band maximum and conduction-band minimum touch at one point in the k space, the Dirac point, which occurs at the Fermi energy. This indicates that graphene is a zero-gap semiconductor. In Fig. 7, we observe that the Fermi energy (the dashed line) is shifted upward with respect to the Dirac point energy, which indicates a charge transfer from TPP to graphene, revealing a n-type doping mechanism. Therefore, graphene would change its electronic characteristic induced by the strong TPP complexation.

As the π-stacking molecule do not alter the graphene atomic structure, their transport properties would be preserved. Similar results have been reported for other aromatic molecules physisorbed on graphene.[34]

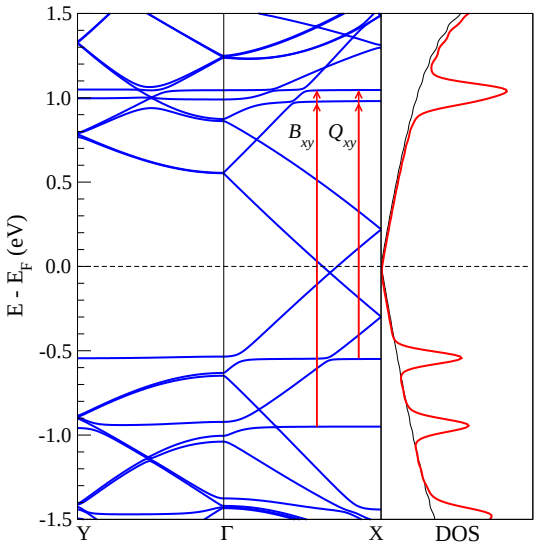

FIG. 7: Band structure and density of states of graphene with a π-stacked TPP represented in a squared reciprocal lattice. The vertical arrows indicate the Q and B transitions between π-stacked TPP frontier orbitals. The black DOS corresponds to pristine graphene.

Figure 8 shows ε_2 of a TPP π-stacked on graphene, The G-TPP compound, considering an in-plain polarizations of incident light. For pristine graphene, we find a strong absorption in the infrared, below 1 eV, and a less intense absorption in the ultraviolet, at around 4 eV, which are attributed to transitions among π and π^* bands. These results are in qualitative agreement with calculated absorption spectra using the GW-BSE approach as well as with experiments,[24,30] unless the redshift previously discussed. For functionalized graphene, we observe two intense absorptions at around 1.57 and 1.96 eV, corresponding to the Q_{xy} and B_{xy} bands of the π-stacked TPP. These peaks show a redshift with respect to those of the isolated TPP of 0.05 eV, which is associated to the distortion of the TPP phenyl groups due to the strong π-stacking interaction. Additional peaks at around 2.6 and 3.1 eV are also associated to the TPP molecule.

IV. SUMMARY AND CONCLUSIONS

We have theoretically investigated the stability and optical absorption properties of a free-base TPP molecule π-stacked on single-walled CNTs, as well as on graphene. 42 CNTs with chiral indices (n,m), where $5 \leq n \leq 12$ and $0 \leq m \leq n$, have been studied. In term of the diameter, they range within $3.9 \leq D \leq 16.6$ Å. The TPP physisorption is described by van der Waals density functional while the optical properties through the imaginary

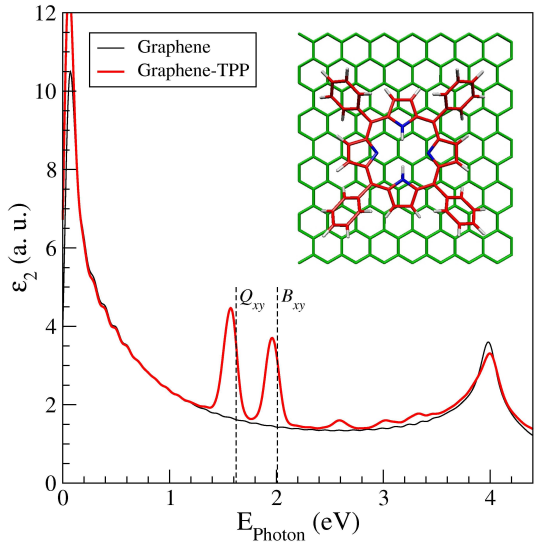

FIG. 8: Imaginary part of the dielectric function for graphene with a π-stacked TPP, for in-plain polarization of the incident light. The dashed lines indicate the Q and B bands of the isolated TPP.

part of the dielectric function in the linear optical response.

We find a strong CNT-TPP π-stacking interaction, with binding energies and adsorption distance varying within $1.1 \leq E_b \leq 1.8$ eV and $3.0 \leq d \leq 3.3$ Å, respectively, where larger E_b and d are obtained for increasing CNT diameters. Our results indicates that diameter instead chirality is the relevant parameter for the strong TPP physisorption, which would be originated in the increasing overlap area between TPP and the CNTs. An upper limit for the CNT-TPP binding strength can be estimated through the TPP physisorption on graphene, which can be viewed as an infinite-diameter CNT. We find very strong π-stacking interactions, with $E_b = 3.32$ eV and $d = 3.42$ Å. However, this strong interaction is not enough to open an energy gap in the functionalized graphene, but it can induce a charge transfer from TPP, suggesting a n-type doping mechanism without compromising the graphene structure and transport properties. Concerning optical properties, we find that Q and B (Soret) TPP absorption bands remain at almost the same energy position after the physisorption on the CNTs, being independent of the CNT structural parameters. Whereas on graphene, the TPP bands show a redshift of about 0.05 eV, which are associated to the distortion of the phenyl groups due to the strong π-stacking interaction. Finally, our results suggest that both compounds CNT-TPP and G-TPP exhibit remarkable stability while preserving the absorption properties of the chromophore, which may be of interest for light-harvesting and bio-labeling applications.

Acknowledgments

This work was supported by the funding agency CONICYT-PIA under the Grant Anillo ACT-1107. JDC acknowledges support from the Universidad de Medellín Research Office through Project No. 684.

[1] Guldi DM, Taieb H, Rahman G, Tagmatarchis N, Prato M (2005) Adv Mater 17:871
[2] Hecht DJ, Ramirez RJA, Briman M, Artukovic E, Chichak KS, Stoddart JF, Grüner G (2006) Nano Lett 6:2031
[3] Mhuircheartaigh EMN, Giordani S, Blau WJ (2006) J Phys Chem B 110:23136
[4] Roquelet C, Garrot D, Lauret JS, Voisin C, Alain-Rizzo V, Roussignol P, Delaire JA, Deleporte E (2010) Appl Phys Lett 97:141918
[5] Malic E, Weber C, Richter M, Atalla V, Klamroth T, Reich PSS, Knorr A (2011) Phys Rev Lett 106:097401
[6] Garrot D, Langlois B, Roquelet C, Michel T, Roussignol P, Delalande C, Delaporte E, Lauret JS, Voisin C (2011) J Phys Chem C 115:23283
[7] Gupta J, Vijayan C, Maurya SK, Goswami D (2011) J Appl Phys 109:113101
[8] Roquelet C, Vialla F, Diederichs C, Roussignol P, Delalande C, Deleporte E, Lauret JS, Voisin C (2012) ACS Nano 6:8796
[9] Barone PW, Baik S, Heller DA, Strano MS (2005) Nature Mater 4:86
[10] Heller DA, et al (2009) Nat Nanotechnol 4:114
[11] Liu Z, Tabakman S, Welsher K, Dai HJ (2009) Nano Res 2:85
[12] Campidelli S, Klumpp C, Bianco A, Guldi DM, Prato M (2006) J Phys Org Chem 19:531
[13] Sprafke JK, Stranks SD, Warner JH, Nicholas RJ, Anderson HL (2011) Ang Chem Int Ed 50:2313
[14] Li H, Zhou B, Lin Y, Gu L, Wang W, Fernando KAS, Kumar S, Allard LF, Sun YP (2004) J Am Chem Soc 126:1014
[15] Lu J, Lai L, Luo G, Zhou J, Qin R, Wang D, Wang L, Mei WN, Li G, Gao Z, Nagase S, Maeda Y, Akasaka T, Yu D (2007) Small 3:1566
[16] Ruiz-Tagle I, Orellana W (2010) Phys Rev B 82:115406
[17] Correa JD, Orellana W (2012) Phys Rev B 86:125417
[18] Correa JD, Orellana W (2013) J Appl Phys 113:174305
[19] Soler JM, Artacho E, Gale JD, García A, Junquera J, Ordejón P, Sánchez-Portal D (2002) J Phys: Condens Mater 14:2745
[20] Dion M, Rydberg H, Schröder E, Langreth DC, Lundqvist BI (2004) Phys Rev Lett 92:246401
[21] Chakarova-Käck SD, Schröder E, Lundqvist BI, Langreth DC (2006) Phys Rev Lett 96:146107
[22] Mak KF, Shan J, Heinz TF (2011) Phys Rev Lett 106:046401
[23] Spataru CD, Ismail-Beigi S, Benedict LX, Louie SG (2004) Phys Rev Lett 92:077402
[24] Yang L, Deslippe J, Park CH, Cohen ML, Louie SG (2009) Phys Rev Lett 103:186802
[25] Weisman RB, Bachilo SM (2003) Nano Lett 3:1235
[26] Kar T, Bettinger HF, Scheiner S, Roy AK (2008) J Phys Chem C 112: 20070
[27] Zacharia R, Ulbricht H, Hertel T (2004) Phys Rev B 69: 155406
[28] Björk J, Hanke F, Palma C-A, Samori P, Cecchini M, Persson M (2010) Phys Chem Lett 1: 3407
[29] Roquelet C, Lauret JS, Alain-Rizzo V, Voisin C, Fleurier R, Delarue M, Garrot D, Loiseau A, Roussignol P, Delaire JA, Deleporte E (2010) Chem Phys Chem 11:1667
[30] Chen Z, Wang XQ (2011) Phys Rev B 83:081405
[31] Gouterman M (1959) J Chem Phys 30:1139
[32] Gouterman M, Wagniere G, Snyder LC (1963) J Mol Spectrosc 11:108
[33] Weiss C, Kobayashi H, Gouterman M (1965) J Mol Spectrosc 16:415
[34] Mao HY, Lu YH, Lin JD, Zhoug S, Wee ATS, Chen W (2013) Prog Surf Sci 88:132